


The abrupt pathological deterioration of cisplatin-induced acute kidney injury: Emerging of a critical time point

Qin Gong^{1,2} | Mulan Wang² | Ya Jiang¹ | Chengliang Zha² | Dong Yu¹ | Fan Lei³ | Yingying Luo^{1,2} | Yulin Feng^{1,2} | Shilin Yang^{1,2} | Jun Li^{1,2}  | Lijun Du^{1,2,3}

¹School of Pharmacy, Jiangxi University of Traditional Chinese Medicine, Nanchang, China

²Pharmacology Laboratory, State Key Laboratory of Innovative Drugs and Efficient Energy-saving Pharmaceutical Equipment, Nanchang, China

³School of Life Sciences, Tsinghua University, Beijing, China

Correspondence

Jun Li, School of Pharmacy, Jiangxi University of Traditional Chinese Medicine, No.56, Yangming Road, Donghu District, Nanchang 330006, Jiangxi Province, China.
Email: 21363492@qq.com

Lijun Du, School of Life Sciences, Tsinghua University, No.30, Shuangqing Road, Haidian District, Beijing 100084, China.
Email: lijundu@mail.tsinghua.edu.cn

Funding information

This research was supported by the National Innovative Drugs 13th Five-Year Major Special Project (grant number 2018ZX09301030-002).

Abstract

Cisplatin (CP), an anticancer drug, often causes kidney damage. However, the mechanism of CP-induced acute kidney injury (AKI) is not completely understood. AKI was induced by intravenous injection (i.v.) of cisplatin at doses of 5, 8, and 10 mg/kg. Anemoside B4 (B4) (20 mg/kg, i.m.) and dexamethasone (DXM) (0.5 mg/kg, i.v.) were used for AKI treatment. Biochemical indicators were assessed using an automatic biochemical analyzer, protein expression was analyzed by western blotting, and morphological changes in the kidney were examined by PAS staining. The serum creatinine (Cre) and blood urea nitrogen (BUN) levels did not change significantly in the first 2 days but abruptly increased on the third day after CP injection. The serum albumin (ALB) and total protein (TP) levels decreased in both a time- and dose-dependent manner. The urine protein level increased, the clearing rate of Cre decreased distinctly, and morphologic changes appeared in a dose-dependent manner. The protein expression of p53/caspase-3, NLRP3, IL-6, and TNF- α was obviously upregulated on day 3; concurrently, nephrin and podocin were downregulated. The expression of LC3II and p62 was upregulated significantly as the CP dose increased. B4 and DXM obviously decreased the BUN and Cre levels after 3 or 5 days of treatment. AKI appeared distinctly in a time-dependent manner at 2 to 5 days after the administration of 5 mg/kg CP and in a dose-dependent manner upon the administration of 5, 8, and 10 mg/kg CP. The third day was a significant time point for renal deterioration, and treatment with B4 and DXM within the first 3 days provided significant protection against AKI.

KEYWORDS

acute kidney injury, anemoside B4, apoptosis, cisplatin, inflammation, therapy

Abbreviations: AKI, acute kidney injury; ALB, albumin; ATN, acute tubular necrosis; BUN, blood urea nitrogen; CP, Cisplatin; Cre, creatinine; DXM, dexamethasone; TP, protein.

Qin Gong and Mulan Wang contributed equally.

This is an open access article under the terms of the Creative Commons Attribution-NonCommercial-NoDerivs License, which permits use and distribution in any medium, provided the original work is properly cited, the use is non-commercial and no modifications or adaptations are made.

© 2021 The Authors. *Pharmacology Research & Perspectives* published by British Pharmacological Society and American Society for Pharmacology and Experimental Therapeutics and John Wiley & Sons Ltd.

1 | INTRODUCTION

Cisplatin (CP) is a nonspecific cytotoxic antitumor drug commonly used in the clinic. It kills tumor cells and causes toxicity to normal cells; for example, renal tubular injury is common and observed as acute renal damage in the clinic.¹⁻³ Studies have shown that the incidence of renal dysfunction after CP use is 3.8% in clinical antitumor practice,⁴ thus, patients using CP are at a higher risk for developing kidney injury (approximately 20%–30%).⁵⁻⁷ Therefore, improving the monitoring of renal function to protect the kidney in a timely manner is the focus of clinical CP chemotherapy.

CP can act directly on the guanine bases of the DNA double-strand, leading to DNA damage and the induction of apoptosis and necrosis.⁸⁻¹⁴ CP specifically acts on renal mitochondrial DNA, causing an ATP energy metabolism disorder that results in kidney injury.¹⁵ In recent years, accumulating studies have reported not only apoptosis and necrosis¹⁶⁻¹⁸ but also autophagy^{19,20} in the kidney after CP treatment. In addition, CP damage in the kidney is also related to multiple mechanisms, such as the PI3K/Akt, JAK/STAT/SOCS, and MAPK signaling pathways.^{21,22}

The mechanism of CP-induced renal impairment is complex. However, there are no reports on the dynamic response to CP from the onset of renal injury. A detailed systematic observation of this process could precisely elucidate the mechanism underlying CP-induced kidney damage and is important for the timely prevention and treatment of CP-induced kidney damage. Therefore, we investigated the dynamic process of CP-induced experimental acute kidney injury (AKI) in rats and the expression of inflammatory apoptotic factors. During the observation, we unexpectedly discovered the key time point of CP-induced renal function damage, as an obvious difference in the renal function index was observed between the second and third days after CP injection. We then conducted experiments to further study this time frame.

2 | MATERIALS AND METHODS

2.1 | Animal treatment and experimental procedure

Male SD rats weighing 160–180 g were purchased from Hunan SJA Laboratory Animal Co., Ltd. (SCXK (Xiang) 2016-0002). This experiment was performed in the Laboratory of Barrier Environment of Jiangxi Bencao-Tiangong Technology Co., Ltd. (SYXK (Gan) 2018-0002). The animals were housed in temperature- and humidity-controlled rooms under a 12 h light/dark cycle and provided unrestricted access to rodent chow and drinking water. All experiments were performed according to the US National Institutes of Health guidelines for humane animal use (NIH publication no. 8023, revised 1978). All procedures described were reviewed and approved by the Institutional Animal Care & Use Committee of Jiangxi University of Traditional Chinese Medicine (TCM) and the Animal Welfare & Ethics Committee of

Jiangxi University of TCM (approval ID: 17-JunLi-B4). The experimental procedure was performed in strict accordance with the guidelines of the Experimental Animal Welfare and Ethics of China.

AKI induced by different doses of CP: Rats were randomly divided into four groups ($n = 10$): the normal group and three CP groups at doses of 5, 8, and 10 mg/kg. The doses of CP were determined according to our previous study.²³ CP (CP, from Jiangsu Hansoh Pharmacy, batch number: 180804) was mixed with normal saline and injected into the tail veins of rats in the CP groups at an injection volume of 5 ml/kg only once, and rats in the normal group were injected with an equal volume of normal saline.

Effect of B4 on AKI: Rats were divided into six groups ($n = 10$): a normal group, model group, model + B4 (5) group (B4 treatment for 5 days), model + B4 (3 + 2) group (B4 treatment for 3 days and no treatment for 2 days), model + DXM (5) group (DXM treatment for 5 days), and model + DXM (3 + 2) group (DXM treatment for 3 days and no treatment for 2 days). CP (5 mg/kg) was intravenously injected to induce AKI. Anemoside B4 was obtained from Prof. YuLin Feng of the Phytochemical Department (batch no. 20161107, 98% purity as determined by HPLC), and 20 mg/kg B4 was administered (i.m. 5 ml/kg). DXM (PubChem CID: 5743), a drug commonly used in clinical immunoinflammatory therapies and often used for AKI,^{24,25} was purchased from Anhui Golden Sun Biochemical Pharmaceutical Co., Ltd. (batch number: 15032521) and dissolved in normal saline (0.5 mg/kg) before being administered via the tail vein (5 ml/kg) after CP administration. The dose was determined according to our previous experiments and as reported by Asayama et al.²⁶

On day 5, rat urine was collected using ZH-B6 metabolite cages (Anhui Zhenghua Biological Instrument Equipment Co., Ltd.). On days 2, 3, and 5, blood samples were collected from the orbital venous plexus on the corresponding days for biochemical analysis. Some rats in each group were anesthetized and euthanized (10% urethane, 10 ml/kg bodyweight, i.p.). Their kidneys were isolated; the right kidney was fixed with 10% formalin for morphological examination, and the left kidney was stored at -80°C for protein expression analysis. Treatment was withdrawn from the remaining rats. On day 14, serum was collected for biochemical analysis, and the kidneys were removed for protein expression analysis.

2.2 | Biochemical analysis

The quantity of urine collected after 24 h was determined, and the protein content was determined. Serum was collected for biochemical analysis. BUN (R1 TG836, R2 TG837), TP (TH619), and ALB (TF126) were all purchased from Japan Pure Pharmaceutical Industry Co., Ltd. Urine protein concentration (CSF) (706061E) and Cre (710241H) were purchased from Beijing Leadman Biochemistry Co., Ltd. Indexes reflecting kidney function were assessed using a 7100 Biochemistry Automatic Analyzer (Hitachi).

2.3 | Histological examination

The kidney tissue was analyzed using a periodic acid Schiff reaction (PAS) staining kit purchased from Leagene Biotechnology Co., Ltd., and the staining was evaluated using a microscope (Leica DM2500). Histological changes attributed to the acute tubular necrosis (ATN) score were quantified by calculating the percentage of tubules that displayed epithelial cell shedding or necrosis, loss of brush border, cast formation, and tubule dilatation as follows: 0 = none; 1 = <10%; 2 = 10%–25%; 3 = 26%–45%; 4 = 46%–75%, and 5 = >75%. Six fields ($\times 200$) were evaluated for each kidney slice.

2.4 | Protein expression

Protein expression was analyzed by western blot as described previously.^{27,28} The kidney tissues were lysed with 2% SDS, and the proteins were separated by 10% sodium dodecyl sulfate-polyacrylamide gel electrophoresis and transferred onto NC membranes. The membranes were blocked with 5% skim milk at room temperature for 2 h and then incubated overnight at 4°C with the following diluted primary antibodies: NF- κ B (rabbit polyclonal antibody, ab16502), TNF- α (rabbit polyclonal antibody, ab6671), NLRP3 (rabbit polyclonal antibody, ab210491), IL-1 β (rabbit polyclonal antibody, ab9722), IL-6 (mouse monoclonal antibody, ab9324), caspase-1 (rabbit polyclonal antibody, ab1872), nephrin (rabbit monoclonal antibody, ab216341) and LC3II (rabbit monoclonal antibody, ab192890) (all from Abcam). Antibodies against ASC (mouse monoclonal antibody, sc-271054), Bcl-2 (mouse monoclonal antibody, sc-56015), and TGF- β 1 (mouse monoclonal antibody, sc-130348) were purchased from Santa Cruz Biotechnology. Antibodies against IL-18 (rabbit polyclonal antibody, TA324190) and podocin (rabbit polyclonal antibody, TA351459) were purchased from Origene, antibodies against p53 (mouse monoclonal antibody, 60283-2-Ig), and p62 (rabbit polyclonal antibody, 18420-1-AP) were purchased from Proteintech, and antibodies against BAX (rabbit polyclonal antibody, 14796), PARP (rabbit polyclonal antibody, 9532T), cleaved PARP (rabbit polyclonal antibody, 94885S) and caspase-3 (rabbit polyclonal antibody, 9662) were purchased from CST. The membranes were incubated with HRP-labeled goat anti-mouse IgG-HRP (ZB2305) and goat anti-rabbit (ZB2301) IgG-HRP secondary antibodies (ZSGB-Bio) at room temperature for 1.5 h, and an ECL solution was used to visualize the target protein bands on an imaging system (Bio-Rad ChemiDocXRS+). ImageJ software was used to quantify the gray levels, and β -actin (mouse monoclonal antibody, TA-09, Zhongshan Jinqiao Biotech Company) was used as an internal control.

2.5 | Statistical analysis

All values are expressed as the mean \pm SEM. Data were statistically analyzed using two-way analysis of variance (ANOVA) followed by post hoc Dunnett's multiple comparison with GraphPad Prism

8.01 software (GraphPad). *p* values below .05 were considered statistically significant. The statistical graph was produced using GraphPad Prism 8.01 software as mentioned above.

3 | RESULTS

3.1 | Kinetic changes in the serum BUN and Cre levels in rats

After an intravenous injection of CP, the BUN and Cre levels in rat serum increased in a dose- and time-dependent manner (Figure 1A,C) and peaked on the fifth day. Notably, the third day after the injection was determined to be a critical time point at which the BUN and Cre levels were markedly increased compared with those on day 2, suggesting that important pathologic changes occurred at that time. This abrupt increase was dose-dependent (Figure 1B,D), and even a small dose of CP (5 mg/kg) caused a significant increase in the BUN and Cre levels on day 3 compared with day 2 after CP injection.

On day 5 after CP injection, the serum ALB level was decreased in a dose-dependent manner, and the renal excretion abilities of the rats were significantly reduced (Figure 2A). The urine protein concentration (CSF) and 24 h urine protein (urine protein = CSF \times urine volume) level were increased, and the 24 h volume of urine was markedly decreased, suggesting that the glomerular membrane was damaged, causing protein leakage (Figure 2B–D). The urine Cre excretion was markedly decreased, and the clearing rate of Cre [Cre clearing rate = (urine volume \times urine Cre)/(serum Cre \times 1440)] was also markedly decreased due only to the urine volume is significantly reduced, indicating that the clearing function of the rat kidneys was reduced after CP injection (Figure 2E,F).

To confirm these pathological changes, we repeated the experiment in CP-injured kidneys. Figure 3 shows that the serum levels of BUN and Cre were significantly increased after CP injection in a time- and dose-dependent manner. Simultaneously, the serum TP and ALB levels were decreased in both a time- and dose-dependent manner. Additionally, day 3 was a notable time point at which the protein levels were decreased significantly compared with those on day 2, especially in the large-dose group (10 mg/kg). All these results indicate that day 3 is a critical time point for CP-induced kidney damage.

3.2 | Expression of protein markers related to apoptosis and inflammation in rat kidneys

To explore the molecular mechanism of CP injury in rat kidneys, we investigated proteins related to apoptosis and inflammation signaling pathways using the western blot assay (Figure 4). The p53 and caspase-3 levels were markedly increased after CP injection, and their levels on day 3 were higher than those on day 2. The expression of p53 peaked on day 5 in the 5 mg/kg group but not in an obvious dose-dependent manner. Caspase-3 expression peaked on day

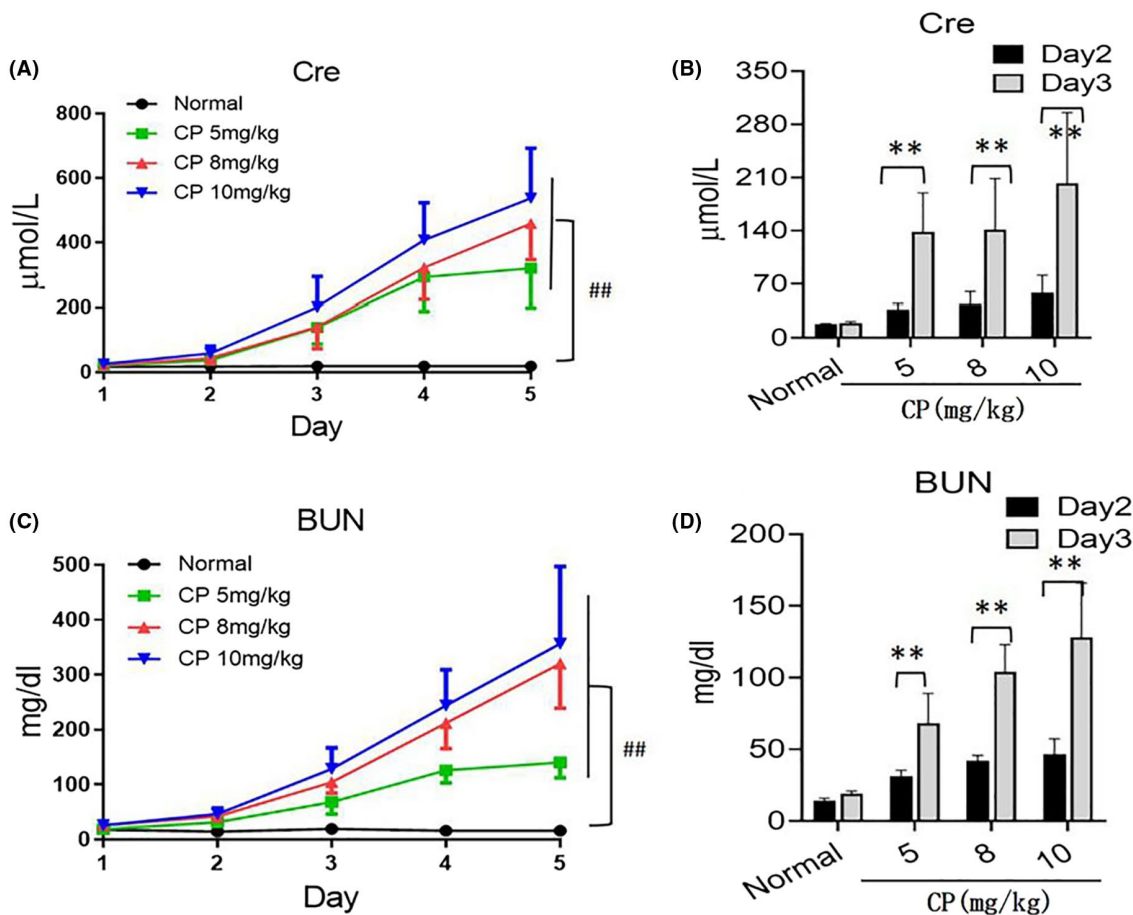


FIGURE 1 Kinetic changes of Cre and BUN of rat acute kidney injury by CP. (A) Linear alteration of Cre at difference days. (B) Difference of Cre between day 2 and day 3 after CP injection. (C) Linear alteration of BUN at difference days. (D) Difference of BUN between day 2 and day 3 after CP injection. The data are shown as mean \pm SEM ($n = 10$). $^{\#}p < .05$, $^{\#\#}p < .01$ versus normal. $^{**}p < .01$ versus day 2

5 in a dose-dependent manner, indicating that caspase-3 responds positively to CP toxicity. Notably, cleaved caspase-3 was expressed at a higher level on day 3 after CP administration, in agreement with the previously described indicators of renal function impairment (Figure 4A–C). Poly (ADP-ribose) polymerase (PARP), another indicator of apoptosis,²⁹ was also expressed at a higher level, and cleaved PARP expression was obviously increased on day 5 in the 5 mg/kg group (Figure 4D,E), supporting that apoptosis was detected in the kidney. The protein expression levels of BAX and Bcl-2 were obviously enhanced on day 3 compared with day 2, but there were no differences in the Bcl-2/BAX ratio, suggesting that the response to CP stress occurred on day 3 (Figure 4F–H). These results confirm that apoptosis occurs even in the early stage of CP administration and that p53-caspase-3 is a major apoptosis pathway.

To determine whether inflammatory cytokines contributed to the acute injury of rat kidneys induced by CP, we investigated the protein expression of nuclear factor- κ B (NF- κ B), TNF- α , and the NLRP3 inflammasome. Figure 5 shows that in the early stage of CP injury, IL-6 and TNF- α were distinctly upregulated, and their levels peaked on day 3 after exposure to CP (Figure 5C,D), indicating that the acute inflammatory reaction was initiated immediately. The expression of NF- κ B was upregulated on day 2 and then decreased

over time but increased as the dose increased, which is worthy of further in-depth study (Figure 5B).

The NLRP3 inflammasome consists of NLRP3, an apoptosis-associated speck-like protein containing a caspase recruitment domain (ASC), caspase-1, interleukin 18 (IL-18), and IL-1 β . The expression of ASC, IL-18, and IL-1 β was obviously upregulated (Figure 5E,F,I), suggesting that the NLRP3 inflammasome was also activated in the pathological AKI induced by CP. Additionally, the expression levels of these proteins peaked on day 3 after CP administration, consistent with those of BUN and Cre, as previously described. Similar to NF- κ B and TNF- α , ASC, IL-18, and IL-1 β were not enhanced in a dose-dependent manner. In addition, NLRP3 was downregulated and caspase-1 was unchanged after the CP injection (Figure 5H,J), which needs to be studied further.

Regarding autophagy markers, the expression of light chain 3 II (LC3II) in rats administered 5 mg/kg CP was lower than that in the normal group within 3 days. However, as the dose increased, the expression of LC3II was significantly increased and was significantly higher than that in the normal group. In addition, the expression of p62 was also significantly increased, suggesting that the induction of autophagy by CP was dose-dependent (Figure 5G,K,L). In the literature, autophagy has been shown to be negatively correlated with

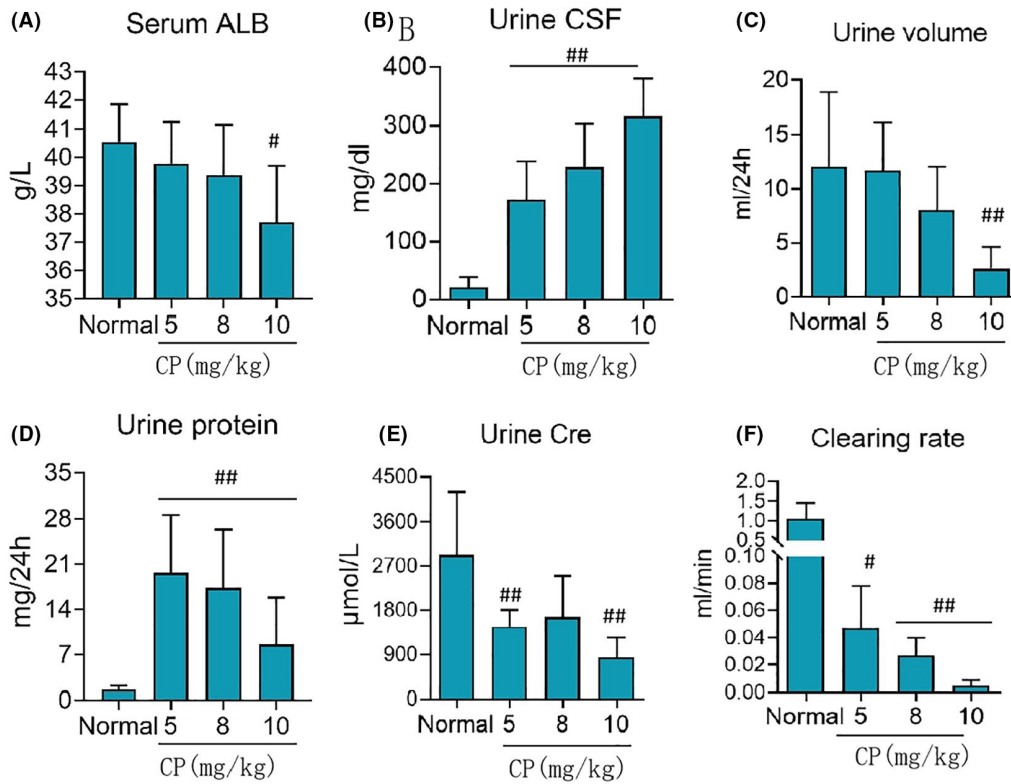


FIGURE 2 (A) The change of albumin (ALB) in rat serum in dose dependent manners. (B–D) The change of 24 h urine protein in dose dependent manners. (E, F) The changes of urine Cre and clearing rate of Cre after CP injection. The changes of kidney index in the urine of acute kidney injury rat induced by CP with different doses. The data are shown as mean \pm SEM ($n = 10$). # $p < .05$, ## $p < .01$ versus normal

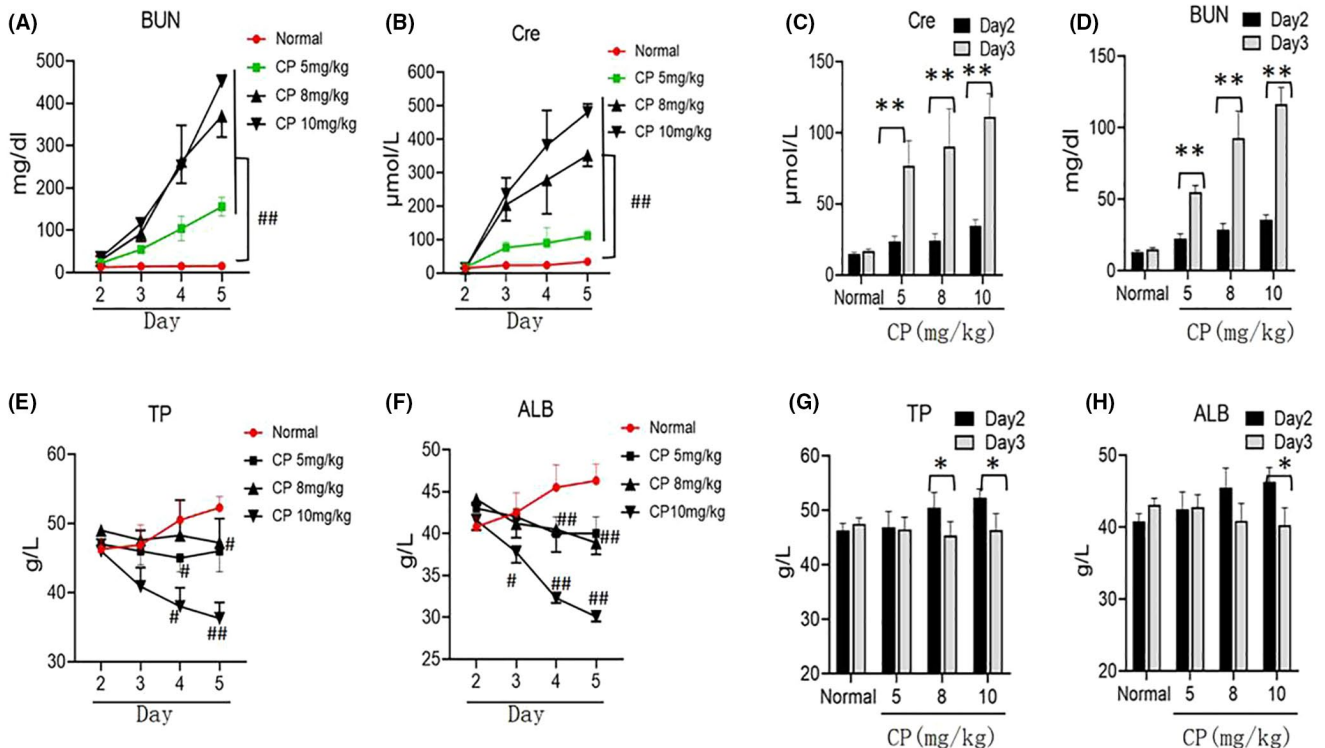


FIGURE 3 Kinetic changes of creatinine (Cre), blood urea nitrogen (BUN), total protein (TP), and albumin (ALB) in rat serum in both time and dose-dependent manners. (A, B) Linear alternation of BUN and Cre after cisplatin (CP) injection. (C, D) Difference of BUN and Cre between day 2 and day 3 caused by CP. (E, F) Linear alternation of TP and ALB after CP injection. (G, H) Difference of TP and ALB between day 2 and day 3 caused by CP. The data are shown as mean \pm SEM ($n = 10$). # $p < .05$, ## $p < .01$ versus normal. * $p < .05$, ** $p < .01$ versus day 2

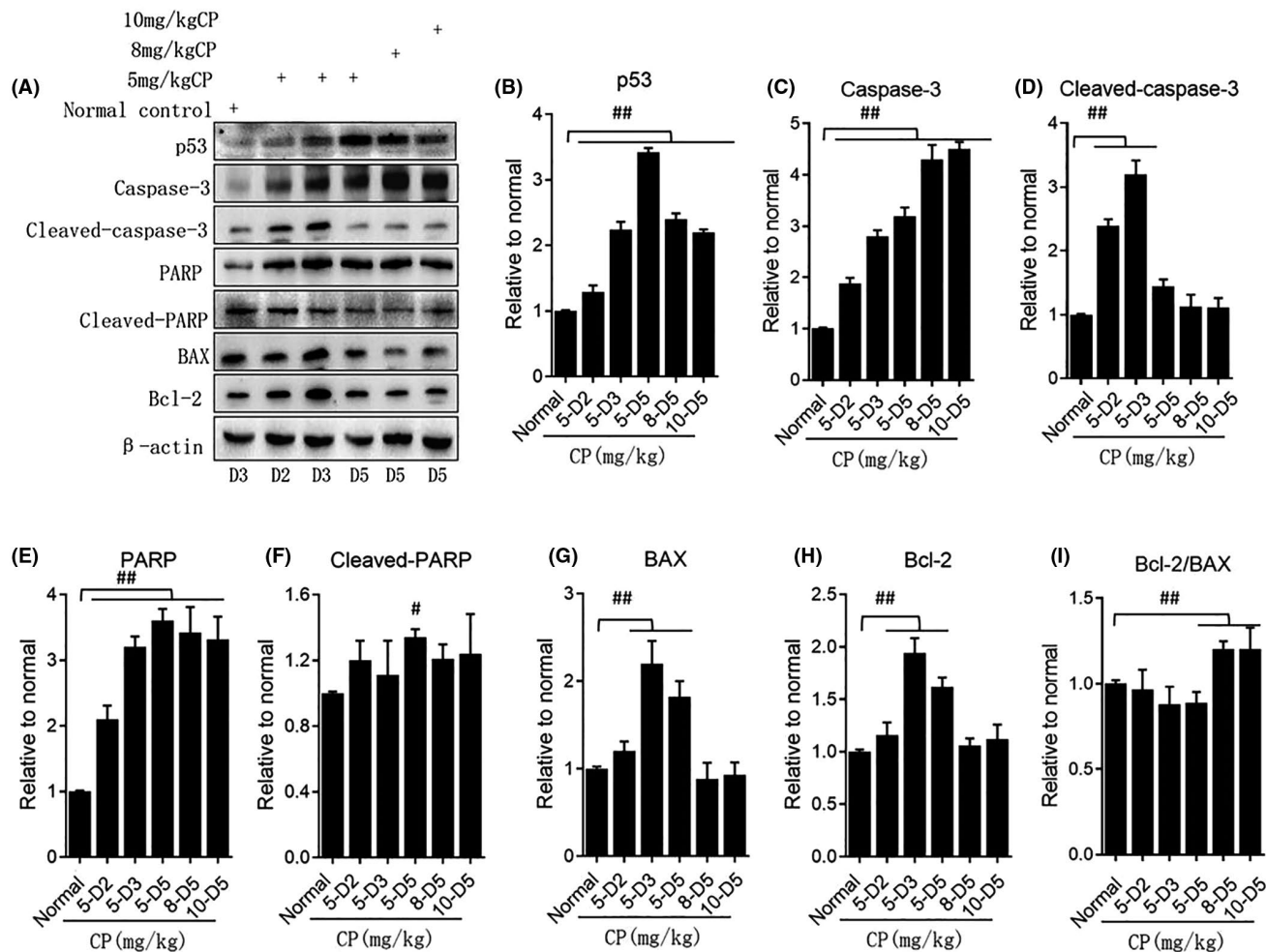


FIGURE 4 Protein expression of apoptosis in rat kidney after injection of cisplatin (CP) with different doses. (A) Western blot assay for detection of the protein expression associated with apoptosis. (B–I) Quantification of the protein expression. The data are shown as mean \pm SEM ($n = 10$). # $p < .05$, ## $p < .01$ versus normal. NS, no significance

NLRP3 expression.^{30,31} Our results did not show a significant correlation, which needs to be further studied.

3.3 | Pathological changes in rat kidneys

Morphological changes in rat kidneys appeared after the CP injection (Figure 6). In the normal group, normal glomeruli and tubular structures were observed. In the day 2 group (5 mg/kg), small amounts of interstitial congestion, partial shedding of renal tubular epithelial cells, and vacuolar degeneration were observed, but protein casts were not. However, in the day 3 group (5 mg/kg), protein casts along with partial tubular dilatation, epithelial cell shedding, and necrosis appeared (Figure 6F). On day 5 after CP administration, the kidney was severely injured, exhibiting hyperemia in the interstitial tissue, renal tubule dilatation, epithelial cell shedding and necrosis, numerous protein casts, and luminal congestion (Figure 6G–L), and the ATN scores were increased in a dose-dependent manner (Figure 6M).

The kidneys of the normal group showed normal glomerular podocytes (Figure 6N), and no obvious glomerular abnormalities

appeared in the rats injected with 5 mg/kg CP on day 2 or day 3 after the injection (Figure 6O,P). However, glomerular podocytes were significantly reduced on day 5, and apoptotic cells appeared (Figure 6Q). Moreover, a significant reduction in podocytes was observed in the glomeruli of the groups in which CP was administered at doses of 8 and 10 mg/kg on day 5 (Figure 6R,S). Protein casts formed in the 10 mg/kg CP group (Figure 6S).

To strengthen the finding of pathological glomerular changes, we measured the protein expression of podocin and nephrin, the major proteins of the renal glomerular basement membrane (Figure 6T). The day after CP administration, podocin expression was significantly downregulated, and the lowest level was observed on the third day. Nephrin expression was downregulated in a dose-dependent manner, which indicated that the podocytes in the glomerular tissue were severely damaged. This result was consistent with the apparent increase in urine protein described previously and indicated that the glomerular basement membrane was damaged at an early time point after CP injection. The expression of podocin in the 10 mg/kg group was higher than that in both the 5 and 8 mg/kg groups, which deserves further study.

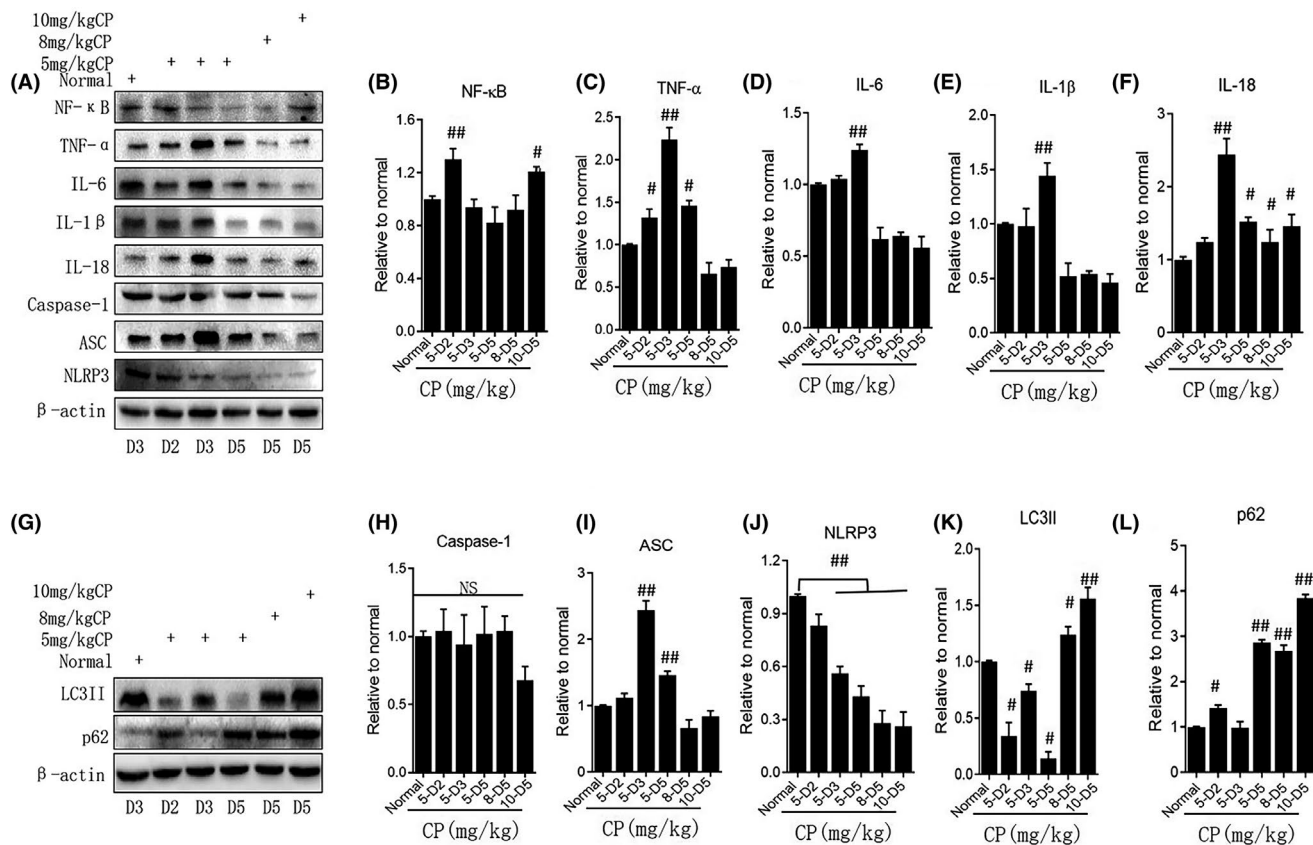


FIGURE 5 Protein expression of inflammation in rat kidney after injection of cisplatin (CP) with different doses. (A, G) Western blot assay for detection of the protein expression. (B-F, H-L) Quantification of the protein expression. The data are shown as mean \pm SEM ($n = 10$). # $p < .05$, ## $p < .01$ versus normal. NS, No significance

3.4 | Determination of the pivotal time point for kidney damage

To confirm the importance of the time frame between day 2 and day 3 in CP-induced kidney damage, we administered CP for different durations (time schedule as in Figure 7A). To compare the groups receiving continuous administration for 5 or 3 days or no treatment for 2 days, blood was collected from the rats on the 5th day, and no significant differences were observed between the groups (Figure 7B,C), suggesting the importance of administering doses on days 2 and 3. Since the BUN and Cre levels were significantly elevated from day 2 to day 3 after CP injection, days 2 and 3 were determined to be critical time points (Figure 7D,E). After treatment on the second and third days, the percentage of Cre increased in the first 2 days and then significantly decreased (Figure 7F,G). On day 14 after drug withdrawal, the serum TP, ALB, BUN, and Cre levels did not significantly differ from those in the normal group (Figure 7H,I). However, the protein expression levels of nephrin and podocin were markedly downregulated, suggesting damage to the podocytes and glomeruli of the kidney despite that CP administration was stopped. At the same time, the expression of transforming growth factor- β 1 (TGF- β 1) was markedly upregulated compared with that in the normal group, implying kidney fibrosis, as TGF- β 1 is known to be critical for fibrosis. B4 enhanced the expression of podocin and nephrin

and suppressed the expression of TGF- β 1, suggesting that B4 can prevent kidney damage and fibrosis after CP injection. The effect of DXM was similar to that of B4 except that it did not enhance podocin expression (Figure 7J-M).

4 | DISCUSSION

This study demonstrates the time point at which acute renal impairment was caused by a single administration of CP. Damage occurred on the third day after CP injection, as the BUN and Cre levels were abruptly increased, accompanied by high expression of apoptotic and inflammatory factors. Treatment with the immunoinflammatory inhibitor DXM and anemosideB4 (a natural small molecule) at this time point can effectively inhibit the changes in BUN and Cre and ameliorate the process of renal deterioration.

Studies have shown that CP mainly binds to DNA containing a GC base pair, causing DNA damage and inducing apoptosis, which is the basic pharmacological principle of the effect of CP on tumors.^{32,33} The induction of apoptosis should be a part of its basic pathophysiological changes. Our results showed that activated caspase-3 levels peaked on the third day and decreased on the fifth day despite that the dose of CP was not increased. However, pro-caspase-3 expression was significantly upregulated in a time- and dose-dependent

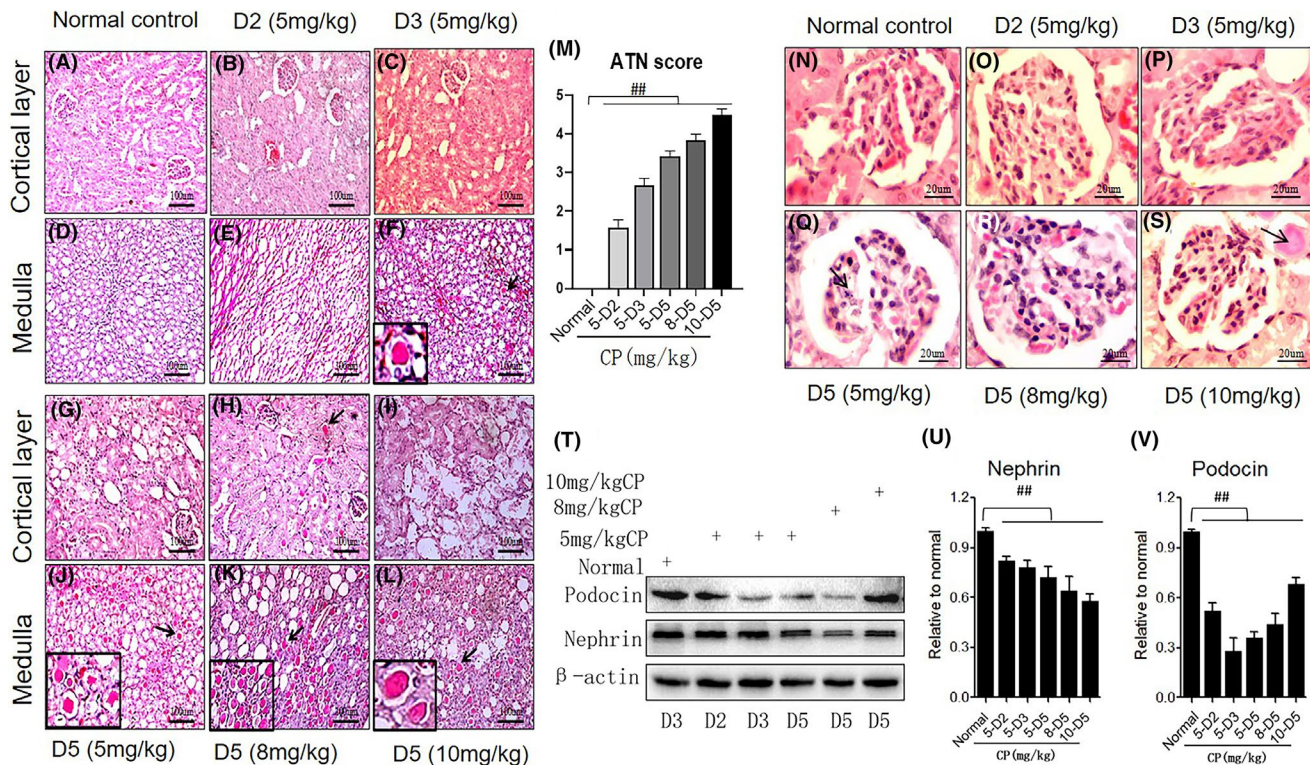


FIGURE 6 Morphology of rat kidney after injection of cisplatin (CP) with different doses. (A–C) Renal cortical layer. (D–F) Renal medulla. (A, D) Normal; (B, E) Day 2 after CP (5 mg/kg); (C, F) Day 3 after CP (5 mg/kg), the arrow indicates protein cast. (G–I) Renal cortical layer. (G, J) Day 5 after CP (5 mg/kg); (H, K) Day 5 after CP (8 mg/kg), the arrow indicates protein cast; (I, L) Day 5 after CP (10 mg/kg), the arrow indicates protein cast, (M) ATN score. (N–S) Glomeruli. (N) Normal; (O) Day 2 after CP (5 mg/kg); (P) Day 3 after CP (5 mg/kg); (Q) Day 5 after CP (5 mg/kg), the arrow indicates apoptotic cells; (R) Day 5 after CP (8 mg/kg); (S) Day 5 after CP (10 mg/kg), the arrow indicates protein cast. (T–V) Protein expressions of podocin and nephrin. (A–L) Amplification of 200 times; (N–S) Amplification of 1000 times. The data are shown as mean \pm SEM ($n = 10$). $^{##}p < .01$ versus normal

manner, indicating the importance of day 3 after CP administration. Correspondingly, the expression of p53 was markedly upregulated. As p53 and caspase-3 are known to act as a switch for the apoptosis pathway,³⁴ this result indicates that upregulation of p53 expression after CP injection activates caspase-3, thereby initiating apoptosis. PARP levels peaked on day 3 after CP administration, which was consistent with that of p53-caspase-3 signaling, confirming that apoptosis occurred.

In addition, an inflammatory response was induced early after CP administration as determined by TNF- α and IL-6 expression, suggesting that the inflammatory response was also triggered upon CP-induced apoptosis. Notably, the expression of ASC and IL-18, which are part of the NLRP3 inflammasome, was significantly increased on day 3 after CP injection, suggesting that the NLRP3 inflammatory complex was also involved in the inflammatory response. Studies have shown that elevated expression of the NLRP3 inflammasome often occurs in chronic inflammatory processes,³⁵ however, our results indicated that NLRP3 was involved in the early AKI process, the stage of apoptosis induced by CP, which suggests that renal tissue damage caused by CP along with the activation of the inflammatory response is a complex pathophysiological process. Thus, the prevention and treatment of CP-induced renal dysfunction in the early stage should be a focus of future studies.

Autophagy is a general term for the process of organelle and cell content degradation by lysosomes.³⁶ Under physiological conditions, autophagy remains at a low level and aims to remove damaged organelles.³⁷ Autophagy activation plays an important role in stabilizing cell morphology and structure and maintaining the normal physiological functions of cells.³⁸ LC3II is a protein marker for autophagy in mammalian cells, and its expression is positively correlated with the level of autophagy.^{39,40} p62 is a binding protein downstream of LC3 and can be regarded as a degradation substrate for autophagy, and its expression is negatively correlated with autophagy levels.⁴¹ Our results showed that LC3II expression was significantly downregulated on day 3 after CP injection, suggesting a decrease in autophagy levels. Moreover, the expression of ASC and IL-18 was significantly increased, while the expression of NLRP3 was decreased. In addition, the levels of other inflammatory factors, such as TNF- α , IL-6, and IL-1 β , were significantly increased, indicating the occurrence of an inflammatory reaction at this time point. However, on the fifth day after CP injection, the autophagy level increased significantly as the CP dose increased and LC3II and p62 were upregulated, which was negatively correlated with the downregulation of NLRP3 expression. Moreover, inflammatory factors were downregulated. The upregulation of both LC3II and p62 expression on the fifth day with increasing CP doses (8 and 10 mg/kg) indicated that autophagy was activated

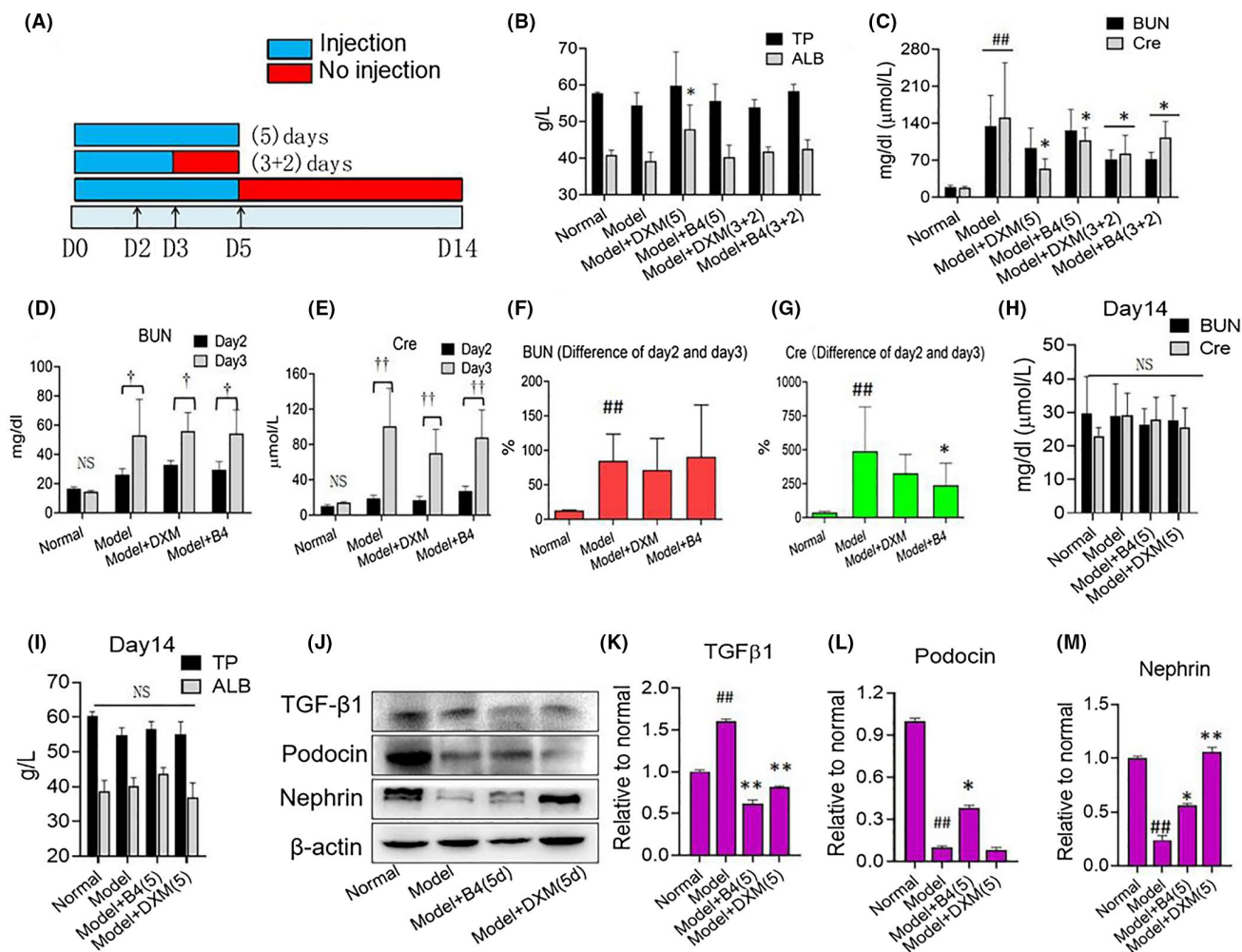


FIGURE 7 Effect of B4 on rat kidney injury induced by cisplatin (CP). (A) Experimental protocol. (B) Serum TP and ALB. (C) Serum BUN and Cre. (D–G) BUN and Cre on day 2 and day 3 after 3 days of drug treatment. (H–M) Serum BUN, Cre, TP, ALB, and protein expression of cytokines of kidney on day 14 with 5 days of drug treatment. DXM, dexamethasone. The data are shown as mean \pm SEM ($n = 5$). # $p < .05$, ## $p < .01$ versus normal. * $p < .05$, ** $p < .01$ versus model group. † $p < .05$, †† $p < .01$ versus day 2. NS, No significance

in a manner by which autophagosomes were both generated and degraded simultaneously, which deserves further study.

Our pathological analyses showed that the renal damage caused by CP appeared mainly in renal tubular epithelial cells, which is in agreement with a previous study.³ Notably, podocytes, an important component of the glomerular basement membrane,⁴² were obviously injured on the second day after CP injection, while the expression of podocin was distinctly downregulated and the apoptosis and inflammatory injury levels peaked on the third day. Podocin was more sensitive to the early damage induced by CP. Nephryn was not as responsive as podocin in the early days after CP treatment. As podocin and nephryn play important roles in the maintenance of renal podocyte and basement membrane integrity,^{43,44} we may conclude that CP impairs renal function, promotes the expression of inflammatory apoptotic factors in renal tissue, and damages the glomerular basement membrane.

Clinically, the dosage of CP generally ranges from 30 to 75 mg/m²,^{45,46} which is equivalent to approximately 5–10 mg/kg in rats.

Our results indicated that AKI was induced at the doses tested and that the damage increased as the dose increased. Therefore, attention should be paid to the protection of renal function in the early stage of CP treatment, especially between days 2 and 3 after CP exposure. We hypothesized that the provision of anti-inflammatory protection shortly after the administration of CP treatment would minimize the renal damage caused by CP. To test this hypothesis, we conducted additional experiments in an attempt to prevent kidney injury induced by CP in the early stage. We used the known anti-inflammatory immunosuppressant DXM, which was administered continuously for 3 days after CP administration and then stopped for 2 days or continuously administered for 5 days. No significant difference in efficacy was observed between continuous administration for 3 days and continuous administration for 5 days as determined by the BUN and Cre levels, suggesting the importance of treatment in the first 3 days. Moreover, this long-term effect also affected the expression of TGF-β1, podocin, and nephryn after CP withdrawal, correlating with renal interstitial fibrosis and the glomerular basement

membrane. This suggests the importance of day 3 after CP administration and of early treatment for the effective prevention of renal damage. In addition to DXM, the natural small molecule B4, which has antitumor and anti-inflammatory activity, had a significant effect on renal damage.⁴⁷⁻⁴⁹ Our results showed that B4 effectively reduced the renal damage caused by CP on the 2nd and 3rd days after CP administration. This result provides valuable information for the in-depth research and clinical application of B4. In our study, male rats were used to observe the time point of CP toxicity and the time window for drug intervention, and whether the estrogen level in female rats would impact our findings remains to be determined.

5 | CONCLUSION

We conducted a systematic investigation of the common clinical problems associated with AKI caused by CP. The results showed that AKI caused by CP was mainly characterized by inflammatory apoptosis, and the third day after CP administration was determined to be a critical time point for disease progression. Controlling this time point and implementing timely therapy should effectively reduce kidney injury.

ACKNOWLEDGEMENTS

We thank all our colleagues in the laboratory for the round-table discussions on the study and for the good suggestions on improving the experiments.

DISCLOSURE

The authors have no potential conflicts of interest to declare.

ETHICS STATEMENT

All experiments were performed according to the US National Institutes of Health guidelines for humane animal use. All procedures described were reviewed and approved by the Institutional Animal Care & Use Committee of Jiangxi University of Traditional Chinese Medicine (TCM) and the Animal Welfare & Ethics Committee of Jiangxi University of TCM (approval ID: 17-JunLi-B4). The experimental procedure was performed in strict accordance with the guidelines of the Experimental Animal Welfare and Ethics of China.

AUTHORS' CONTRIBUTIONS

Shilin Yang, Lijun Du, and Yulin Feng conceptualized the study; Qin Gong, Jun Li, and Lijun Du designed the experiments; Qin Gong, Ya Jiang, Fei Lei, Mulan Wang, and Chengliang Zha performed the experiments; Qin Gong, Jun Li, Yingying Luo, and Lijun Du analyzed the experimental data; and Dong Yu, Qin Gong, Jun Li, Mulan Wang, and Lijun Du wrote the paper. All authors read and approved the final manuscript.

DATA AVAILABILITY STATEMENT

All data generated and analyzed in the study are available from the corresponding author upon reasonable request.

ORCID

Jun Li  <https://orcid.org/0000-0002-2868-9511>

REFERENCES

- Almanric K, Marceau N, Cantin A, Bertin É. Risk factors for nephrotoxicity associated with cisplatin. *Can J Hosp Pharm.* 2017;70:e99-e106.
- Higuchi K, Yanagawa T. Evaluating dose of cisplatin responsible for causing nephrotoxicity. *PLoS One.* 2019;14:e0215757.
- Manohar S, Leung N. Cisplatin nephrotoxicity: a review of the literature. *J Nephrol.* 2018;31:15-25.
- Dhillon P, Amir E, Lo M, et al. A case-control study analyzing mannitol dosing for prevention of cisplatin-induced acute nephrotoxicity. *J Oncol Pharm Pract.* 2019;25:875-883.
- Driessen CM, Ham JC, Loo M, et al. Genetic variants as predictive markers for ototoxicity and nephrotoxicity in patients with locally advanced head and neck cancer treated with cisplatin-containing chemoradiotherapy (The prone study). *Cancers.* 2019;11:e551.
- Duffy EA, Fitzgerald W, Boyle K, Rohatgi R. Nephrotoxicity: evidence in patients receiving cisplatin therapy. *Clin J Oncol Nurs.* 2018;22:175-183.
- El Hamamsy M, Kamal N, Bazan NS, El Haddad M. Evaluation of the effect of acetazolamide versus mannitol on cisplatin-induced nephrotoxicity, a pilot study. *Int J Clin Pharm.* 2018;40:1539-1547.
- Davies MS, Berners-Price SJ, Hambley TW. Rates of platination of AG and GA containing double-stranded oligonucleotides: insights into why cisplatin binds to GG and AG but not GA sequences in DNA. *J Am Chem Soc.* 1998;120:11380-11390.
- Lin X, Kim HK, Howell SB. The role of DNA mismatch repair in cisplatin mutagenicity. *J Inorg Biochem.* 1999;77:89-93.
- Pil PM, Lippard SJ. Specific binding of chromosomal protein HMG1 to DNA damaged by the anticancer drug cisplatin. *Science.* 1992;256:234-237.
- Takahara PM, Frederick CA, Lippard SJ. Crystal structure of the anticancer drug cisplatin bound to duplex DNA. *J Am Chem Soc.* 1996;118:12309-12321.
- Takahara PM, Rosenzweig AC, Frederick CA, Lippard SJ. Crystal structure of double-stranded DNA containing the major adduct of the anticancer drug cisplatin. *Nature.* 1995;377:649-652.
- Tsunekawa M, Wang S, Kato T, Yamashita T, Ma N. Taurine administration mitigates cisplatin induced acute nephrotoxicity by decreasing DNA damage and inflammation: an immunocytochemical study. *Adv Exp Med Biol.* 2017;975:703-716.
- Zazuli Z, Vijverberg S, Slob E, et al. Genetic variations and cisplatin nephrotoxicity: a systematic review. *Front Pharmacol.* 2018;9:e1111.
- Maniccia-Bozzo E, Bueno Espiritu M, Singh G. Differential effects of cisplatin on mouse hepatic and renal mitochondrial DNA. *Mol Cell Biochem.* 1990;94:83-88.
- Du B, Dai XM, Li S, et al. MiR-30c regulates cisplatin-induced apoptosis of renal tubular epithelial cells by targeting Bnip3L and Hspa5. *Cell Death Dis.* 2017;8:e2987.
- Gao L, Liu MM, Zang HM, et al. Restoration of E-cadherin by PPBICA protects against cisplatin-induced acute kidney injury by attenuating inflammation and programmed cell death. *Lab Invest.* 2018;98:911-923.
- Yang Y, Fu Y, Wang P, et al. Intervention of mitochondrial activity attenuates cisplatin-induced acute kidney injury. *Int Urol Nephrol.* 2019;51:1207-1218.
- Shen Q, Zhang X, Li Q, et al. TLR2 protects cisplatin-induced acute kidney injury associated with autophagy via PI3K/Akt signaling pathway. *J Cell Biochem.* 2019;120:4366-4374.
- Yang C, Kaushal V, Shah SV, Kaushal GP. Autophagy is associated with apoptosis in cisplatin injury to renal tubular epithelial cells. *Am J Physiol Renal Physiol.* 2008;294:F777-F787.

21. Sahu AK, Verma VK, Mutneja E, et al. Mangiferin attenuates cisplatin-induced acute kidney injury in rats mediating modulation of MAPK pathway. *Mol Cell Biochem*. 2019;452:141-152.
22. Tsogbadrakh B, Ryu H, Ju KD, et al. AICAR, an AMPK activator, protects against cisplatin-induced acute kidney injury through the JAK/STAT/SOCS pathway. *Biochem Biophys Res Commun*. 2019;509:680-686.
23. Gong Q, Yin JL, Wang ML, et al. Comprehensive study of dexamethasone on albumin biogenesis during normal and pathological renal conditions. *Pharm Biol*. 2020;58:1252-1262.
24. Chen Y, Du YW, Li Y, et al. Panaxadiol saponin and dexamethasone improve renal function in lipopolysaccharide-induced mouse model of acute kidney injury. *PLoS One*. 2015;7:e0134653.
25. Kumar S, Allen DA, Kieswich JE, et al. Dexamethasone ameliorates renal ischemia-reperfusion injury. *J Am Soc Nephrol*. 2009;11:2412-2425.
26. Asayama K, Hayashibe H, Dobashi K, Uchida N, Kato K. Effect of dexamethasone on antioxidant enzymes in fetal rat lungs and kidneys. *Neonatology*. 1992;62:136-144.
27. Wang XP, Yu X, Yan XJ, et al. TRPM8 in the negative regulation of TNF- α expression during cold stress. *Sci Rep*. 2017;7:e45155.
28. Yu X, Wang XP, Lei F, et al. Pomegranate leaf attenuates lipid absorption in the small intestine in hyperlipidemic mice by inhibiting lipase activity. *Chin J Nat Med*. 2017;15:732-739.
29. Liu H, He Z, Bode P, MochH SHU. Downregulation of autophagy-related proteins 1, 5, and 16 in testicular germ cell tumors parallels lowered LC3B and elevated p62 levels, suggesting reduced basal autophagy. *Front Oncol*. 2018;8:e366.
30. Pun NT, Park PH. Role of p62 in the suppression of inflammatory cytokine production by adiponectin in macrophages: involvement of autophagy and p21/Nrf2 axis. *Sci Rep*. 2017;7:e456.
31. Qu XY, Gao H, Tao LN, et al. Autophagy inhibition-enhanced assembly of the NLRP3 inflammasome is associated with acisplatin-induced acute injury to the liver and kidneys in rats. *J Biochem Mol Toxicol*. 2019;33:e22208.
32. Hemminki K, Thilly WG. Binding of cisplatin to specific sequences of human DNA in vitro. *Mutat Res*. 1988;202:133-138.
33. Reed E, Ozols RF, Tarone R, Yuspa SH, Poirier MC. The measurement of cisplatin-DNA adduct levels in testicular cancer patients. *Carcinogenesis*. 1988;9:1909-1911.
34. Liu C, Vojnovic D, Kochevar IE, Jurkunas UV. UV-A irradiation activates Nrf2-regulated antioxidant defense and induces p53/caspase-3-dependent apoptosis in corneal endothelial cells. *Invest Ophthalmol Vis Sci*. 2016;57:2319-2327.
35. Gurung P, Li B, Subbarao Malireddi RK, Lamkanfi M, Geiger TL, Kanneganti TD. Chronic TLR stimulation controls NLRP3 inflammasome activation through IL-10 mediated regulation of NLRP3 expression and caspase-8 activation. *Sci Rep*. 2015;5:e14488.
36. Wollert T. Autophagy. *Current Biol*. 2019;29:R671-R677.
37. Galluzzi L, Green DR. Autophagy-independent functions of the autophagy machinery. *Cell*. 2019;177:1682-1699.
38. Lamb CA, Yoshimori T, Tooze SA. The autophagosome: origins unknown, biogenesis complex. *Nat Rev Mol Cell Biol*. 2013;14:759-774.
39. Liu X, Kang J, Wang H, Huang T. Mitochondrial ROS contribute to oridonin-induced HepG2 apoptosis through PARP activation. *Oncol Lett*. 2018;15:2881-2888.
40. Wei Y, Ren J, Luan Z, Wang Y. Effects of various autophagy modulators on the expression of autophagic markers LC3II and p62. *J Chin Pharm Univ*. 2018;49:341-347.
41. Xu Y, Zhang J, Tian C, et al. Overexpression of p62/SQSTM1 promotes the degradations of abnormally accumulated PrP mutants in cytoplasm and relieves the associated cytotoxicities via autophagy-lysosome-dependent way. *Med Microbiol Immunol*. 2014;203:73-84.
42. Tofighi A, Ahmadi S, Seyyedi SM, Shirpoor A, Kheradmand F, Gharalari FH. Nandrolone administration with or without strenuous exercise promotes overexpression of nephrin and podocin genes and induces structural and functional alterations in the kidneys of rats. *Toxicol Lett*. 2018;282:147-153.
43. New LA, Martin CE, Scott RP, et al. Nephrin tyrosine phosphorylation is required to stabilize and restore podocyte foot process architecture. *J Am Soc Nephrol*. 2016;27:422-4235.
44. Qi XM, Wang J, Xu XX, Li YY, Wu TG. FK506 reduces albuminuria through improving podocyte nephrin and podocin expression in diabetic rats. *Inflam Res*. 2016;65:103-114.
45. Ibrahim ME, Chang C, Hu Y, et al. Pharmacokinetic determinants of cisplatin-induced subclinical kidney injury in oncology patients. *Eur J Clin Pharmacol*. 2019;75:51-57.
46. Scagliotti GV, Gaafar R, Nowak AK, et al. Nintedanib in combination with pemetrexed and cisplatin for chemotherapy-naive patients with advanced malignant pleural mesothelioma (LUME-Meso): a double-blind, randomised, placebo-controlled phase 3 trial. *Lancet Respir Med*. 2019;7:569-580.
47. He LL, Gong Q, Wang ML, et al. Anemoside B4 protects rat kidney from adenine-induced injury by attenuating inflammation and fibrosis and enhancing podocin and nephrin expression. *Evid Based Complement Alternat Med*. 2019;2019:e8031039.
48. He LL, Gong Q, Yu X, et al. Proteomic changes in rat kidney injured by adenine and the regulation of anemoside B4. *J Chin Pharm Sci*. 2019;28:10-20.
49. Xue S, Zhou Y, Zhang J, et al. Anemoside B4 exerts anti-cancer effect by inducing apoptosis and autophagy through inhibition of PI3K/Akt/mTOR pathway in hepatocellular carcinoma. *Am J Transl Res*. 2019;11:2580-2589.

How to cite this article: Gong Q, Wang M, Jiang Y, et al. The abrupt pathological deterioration of cisplatin-induced acute kidney injury: Emerging of a critical time point. *Pharmacol Res Perspect*. 2021;9:e00895. doi:[10.1002/prp2.895](https://doi.org/10.1002/prp2.895)